Cell, Vol. 81, 95–105, April 7, 1995, Copyright © 1995 by Cell Press

Mutations in *aurora* Prevent Centrosome Separation Leading to the Formation of Monopolar Spindles

David M. Glover, Mark H. Leibowitz, Doris A. McLean, and Huw Parry*
Cancer Research Campaign Cell Cycle Genetics Group
Department of Anatomy and Physiology
Medical Sciences Institute
University of Dundee
Dundee DD1 4HN
Scotland

Summary

We show that female sterile mutations of *aurora* (*aur*) are allelic to mutations in the lethal complementation group *ck*^{10}. This lies in a cytogenetic interval, 87A7-A9, that contains eight transcription units. A 250 bp region upstream of both *aur* and a divergent transcription unit corresponds to the site of a specific chromatin structure (scs') previously proposed to be a barrier to insulate enhancers of the major *hsp70* gene at 87A7. Syncytial embryos derived from *aur* mothers display closely paired centrosomes at inappropriate mitotic stages and develop interconnected spindles in which the poles are shared. Amorphic alleles result in pupal lethality and in mitotic arrest in which condensed chromosomes are arranged on circular monopolar spindles. The size of the single centrosomal body in these circular figures suggests that loss of function of the serine-threonine protein kinase encoded by *aur* leads to a failure of the centrosomes to separate and form a bipolar spindle.

Introduction

The animal cell centrosome comprises a mother–daughter centriole pair together with surrounding pericentriolar material that nucleates cytoplasmic microtubules in interphase and spindle microtubules during mitosis. In most cells, centriole duplication occurs during G1, but the centrioles remain associated within a single functional unit that separates into two at the onset of mitosis (reviewed by Vandre and Borisy, 1989). The entry into mitosis is mediated by the p34^{cdc2} kinase and its associated cyclin subunits (reviewed by Nurse, 1990). This activity brings about the breakdown of the nuclear envelope, chromosome condensation, the dissociation of cytoplasmic microtubules, and their replacement by astral arrays of microtubules. Verde et al. (1990) have shown that the associated changes in microtubule dynamics are regulated by the p34^{cdc2} kinase. Centrosome separation can be initiated either before or after nuclear envelope breakdown and destruction of cytoplasmic microtubules, suggesting that its regulation may be independent of p34^{cdc2} activation. The potential of the centrosome cycle to take place autonomously of other cell cycle events is even more striking in the embryonic development of several species. Thus, centrosome duplication continues in Xenopus embryos treated with cycloheximide in which other cell cycle events cannot take place because of the failure to synthesize the mitotic cyclins (Gard et al., 1990). Autonomous replication of centrosomes has been seen in the embryos of sea urchins in the absence of protein synthesis (Sluder et al., 1990), in starfish and Drosophila embryos in the absence of DNA synthesis (Nagano et al., 1981; Raff and Glover, 1988), and in sea urchin or starfish embryos in the absence of nuclei (Sluder and Lewis, 1986; Picard et al., 1988). In the rapid mitotic cycles of the syncytial Drosophila embryo that do not have gap phases, centriole separation begins at metaphase within the two centrosomes at the spindle poles (Callaini and Riparbelli, 1990). These split at telophase into two centrosomes, each containing a single centriole that is duplicated in the following interphase. The centriole cycle has not been studied in detail at later developmental stages of Drosophila when distinct G1 and G2 phases are introduced into the cell cycle.

We have undertaken a search for mutations that affect the centrosome cycle in Drosophila. As abnormal centrosome behavior in the syncytial embryo appears to be a secondary consequence of a large number of mitotic mutants in Drosophila, it is important to analyze centrosome behavior at other developmental stages. This is often possible by analyzing an allelic series of mutant alleles at a particular locus. Maternal-effect mutations leading to abnormal nuclear division cycles in the syncytial embryo can occur in genes encoding proteins apparently required only for this stage, as, for example, the mutation *giant nuclei* (*gnu*) (Freeman et al., 1986), or they may represent weak mutant alleles of genes that are also required at later developmental stages, as, for example, *polo* (Sunkel and Glover, 1988). *polo* was identified through a maternal-effect mutation that leads homozygous mutant females to produce syncytial embryos that have severe mitotic abnormalities. Homozygous mutant larvae display abnormal mitoses in larval neuroblasts and abnormal meiotic divisions. Nevertheless, these cell cycle defects are not sufficient to prevent further development, and adults are produced that have reduced fertility and that display meiotic nondisjunction (Sunkel and Glover, 1988). On the other hand, stronger mutant alleles of *polo* do result in larval lethality and thus exemplify a general mutant phenotype indicative of defects in the proliferation of imaginal tissues (Szabad and Bryant, 1982; Gatti and Baker, 1989). Drosophila homozygous for these mutations can survive through embryogenesis to later stages of development because the gene products required for the early nuclear divisions are provided by the heterozygous mother. *polo* encodes a serine–threonine protein kinase that would appear to be a stable protein, suggesting that its cyclical activity might be regulated by posttranslational modifications such as phosphorylation (Llamazares et al., 1991; Fenton and Glover, 1993).

*Present address: John Innes Institute, Colney Lane, Norwich NR4 7UH, England.

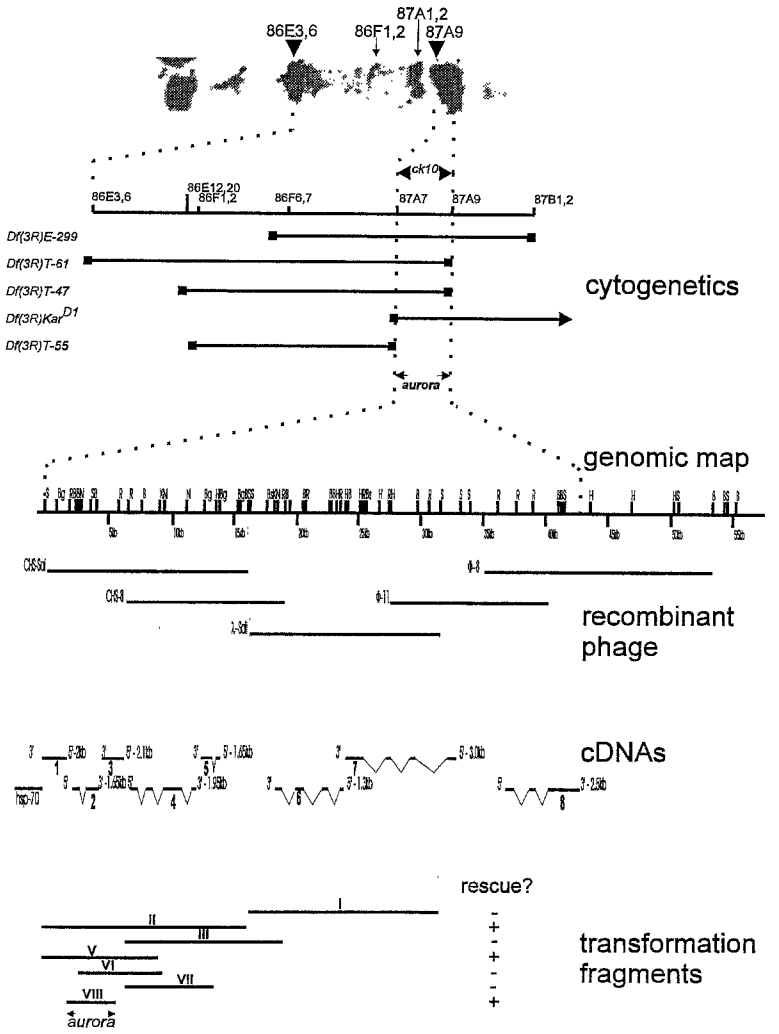

Figure 1. Cytological and Molecular Maps of the 86E-87A Region Showing the Localization of *aur*

(Micrograph) This shows a segment of salivary gland chromosome arm 3R from a wild-type larva. It has been hybridized with a ^{3}H-thymidine-labeled cloned 13 kb SalI fragment containing the breakpoint of *Df(3R)T-61*, resulting in the deposition of silver grains at 86E3-6 and 87A9.

(Cytogenetics) The cytological extents of the indicated five deficiencies are shown in relation to the salivary gland chromsome map, together with their ability to uncover the female sterility of *aur*^{287}. The upper four deficiencies shown on the diagram are able to uncover *aur* whereas the lower one cannot. This places *aur* at 87A7-9. The deficiency chromosomes used for cytological mapping have the following breakpoints: *Df(3R)KarD*^{1}, 87A7 to 87D1-2 (Caggese et al., 1979); *Df(3R)T-61*, 86E3-6 to 87A9 (C. Gonzalez, personal communication); *Df(3R)T-47*, 86E12-20 to 87A9 (Gausz et al., 1981); *Df(3R)T-55*, 87F1-2 to 87A7 (Gausz et al., 1981); *Df(3R)E-229*, 87F6-7 to 87B1-2 (Ish-Horowicz et al., 1979).

(Genomic map) A compilation of the restriction endonuclease cleavage maps of all phage in the chromosomal walk. The 87A7 breakpoint of *Df(3R)KarD*^{1} was determined by Ish-Horowicz and Pinchin (1980). Identification of the distal breakpoint of *Df(3R)T-61* is described in Results and Experimental Procedures. Restriction sites are represented as follows: B, BamHI; Bg, BglII; Bs, BstI; H, HindIII; K, KpnI; N, NcoI; R, EcoRI; S, SalI; X, XbaI.

(Recombinant phage) The indicated phage (see Experimental Procedures) are shown aligned against the genomic molecular map.

(cDNAs) The cDNAs *87A7-9/1* to *87A7-9/8* were isolated from an early embryonic cDNA library (Brown and Kafatos, 1988) by screening with probes from the recombinant phage. The positions of introns within these gene has not been accurately determined, but is deduced by comparison of the restriction maps of cDNA and genomic clones and from the results of Southern blot analysis of labeled cDNAs to digests of the recombinant phage. The 5′ and 3′ ends of these cDNAs were orientated with respect to the genome by making use of the unique restriction sites that exist in pNB40. The lengths of the cDNAs are indicated in kilobases.

(Transformation fragments) Horizontal bars indicate the extents of the restriction endonuclease cleavage fragments introduced into pW8 for transformation (constructs I–VIII; see Experimental Procedures).

Several maternal-effect mutations have been described in which free centrosomes are seen in the cytoplasm of syncytial embryos (Freeman et al., 1986; Gonzalez et al., 1990; Sullivan et al., 1990; Vessey et al., 1991; Girdham and Glover, 1991). In many cases this seems to be a secondary consequence of another cell cycle defect, for example, uncontrolled DNA replication in the case of *gnu* (Freeman et al., 1986). It probably reflects the ease with which the centrosome cycle can be uncoupled from other mitotic events in syncytial embryos (Raff and Glover, 1988). Other mutations cause aberrant centrosome behavior in larval neuroblasts that are specific to the mutant gene under study. *abnormal spindle* (*asp*), for example, leads to metaphase arrest in such cells, many of which have a single centrosome nucleating an asymmetric array of microtubules on a hemispindle (Ripoll et al., 1985; Gonzalez et al., 1990). Mutation in *merry-go-round* (*mgr*) results in the formation of circular monopolar spindles in larval neuroblasts (Gonzalez et al., 1988; C. Gonzalez, unpublished data), and similar structures are seen as a result of mutation in a gene encoding a kinesin-like protein at 61F (Heck et al., 1993). In this paper we describe the failure of centrosome separation in the division cycles in both syncytial embryos and larval neuroblasts that results from loss of function of a gene encoding a putative serine–threonine protein kinase. We discuss the role of this enzyme in the centrosome duplication–separation cycle in relation to other genes with similar mutant phenotypes.

Results

Mutant Alleles of *aurora*

We first identified mutations in the gene *aurora* (*aur*) while screening the phenotypes of embryos derived from a collection of recessive female sterile mutants isolated in the laboratory of C. Nüsslein-Volhard (Tearle and Nüsslein-

Table 1. Complementation Tests on *ck10* and *aur* Chromosomes

	$ck10^{e209}$	$ck10^{e200}$	$ck10^{e170}$	$ck10^{e160}$	$ck10^{hs55}$	$Df(3R)KarD^{1}$	*Df(3R)T-61*	aur^{287}
$ck10^{e209}$	3	P	P	fs	P	P	P	fs
$ck10^{e200}$		3	P	fs	P	P	P	fs
$ck10^{e170}$			E	fs	P	P	E	fs
$ck10^{e160}$				P	fs	P	fs	fs
$ck10^{hs55}$					E	E	P	fs
$Df(3R)KarD^{1}$						E	P	fs
Df(3R)T-61							E	fs
aur^{287}								fs

The lethal stage is indicated as follows: E, embryonic lethal; 3, third instar larval lethal; P, pupal lethal. Female sterility is indicated as fs.

Volhard, 1987; Lindsley and Zimm, 1992). Embryos derived from females homozygous for each of the three mutant alleles, $aur^{287\text{-}19}$, $aur^{074\text{-}18}$, and $aur^{175\text{-}5}$, each showed similar mitotic defects observed by staining chromosomes using the fluorescent dye Hoechst 33258 (see below). We localized *aur* between *Lyra* (*Ly*) and *Stubble* (*Sb*) to 50.1 map units and then tested a series of deficiencies that remove segments of the right arm of chromosome 3 for their ability to uncover the *aur* mutation (Figure 1). This located the *aur* gene between the proximal breakpoint of $Df(3R)KarD^{1}$, which disrupts the distal *hsp70* gene at 87A7 (Ish-Horowicz and Pinchin, 1980), and the distal breakpoint shared at the cytological level by *Df(3R)T-61* and *Df(3R)T-47*.

A saturation screen has been previously carried out to look for ethyl methanesulfonate–generated lethal mutations falling within the interval 86F1-2 to 87B15 (Gausz et al., 1981). These workers identified one lethal complementation group, ck^{10}, within the same cytological interval to which we now map the female sterile *aur* mutations. Five pupal lethal alleles, e^{170}, e^{200}, e^{209}, e^{132}, and hs^{55}, and one female sterile allele, e^{160}, were identified in this study. Complementation tests between $aur^{287\text{-}19}$ alleles showed that none of the five available ck^{10} alleles was able to complement the *aur* mutation and that in all cases the heterozygotes were sterile (Table 1; see Experimental Procedures). Thus, the *aur* locus corresponds to the lethal complementation group in the interval 87A8-9. When the aur^{ck10} alleles were placed in heterozygous combinations among themselves, the mutants died at the pupal stage, with the exception of aur^{e160}, which resulted in sterility rather than lethality. It should be noted that the aur^{e160} chromosome and several of the other chromosomes carrying *aur* alleles carry additional mutations outside 87A8-9 (see Experimental Procedures). Lethality at the white pupal stage was a common phenotype shown by four of these alleles placed over deficiencies extending either proximally or distally to the interval. The double deficiency heterozygote $Df(3R)KarD^{1}$/Df(3R)T-61 also dies at the white pupal stage and has an identical mitotic phenotype to that shown by any one of this group of four alleles when hemizygous (see below), leading us to suggest that four of the five $aur^{ck10(3)}$ alleles are amorphic mutations.

aur Is One of Eight Transcription Units within an Interval That Has One Identified Lethal Complementation Group

The locus was cloned via chromosome walking from the well-characterized heat shock locus at 87A7. The breakpoint that defines the proximal boundary of the 87A7-9 region was already cloned (Ish-Horowicz and Pinchin, 1980). A. Udvardy (Szeged) gave us two plasmids, CHS-Sal and CHS-8, that together extend 15 kb distally from *hsp70*. These provided an entry point from which we continued to walk (see Experimental Procedures). To determine whether our walk had reached the distal breakpoint of *Df(3R)T-61* that defines the distal limit of the interval, we used cloned fragments of wild-type genomic DNA to probe Southern blots of DNA from both wild-type and *Df(3R)T-61*/+ flies. In this way, a 13 kb SalI fragment was identified that was unique to the *Df(3R)T-61* chromosome. This fragment was cloned from the *Df(3R)T-61* chromosome and found to hybridize in situ to 87A9 and 86E3-6 on wild-type polytene chromosomes, in agreement with the cytological limits of *Df(3R)T-61* (Figure 1).

As the *aur* gene product is maternally provided to embryos, we chose to identify cDNAs from an early embryonic cDNA library corresponding to transcribed genomic sequences within the cloned interval (see Experimental Procedures). Using fragments of genomic DNA spanning the region between the *Df(3R)T-61* and $Df(3R)KarD^{1}$ breakpoints we isolated eight unique cDNAs of varying sizes (*87A7-9/1* to *87A7-9/8*; Figure 1). These were positioned against a restriction map of the genomic interval using a combination of Southern blotting and comparative restriction mapping (Figure 1). Thus, whereas saturation mutagenesis by Gausz et al. (1981) defined only a single lethal complementation group, our molecular studies indicate the presence of at least eight transcription units.

Germline transformation experiments identified which transcription unit within the 87A7-9 genomic interval corresponded to the *aur* locus. Specific genomic DNA fragments were tested for their ability to rescue *aur* mutations (Figure 1; see Experimental Procedures), and, by process of elimination, a minimal rescuing fragment was identified in construct VIII. This contains the entire transcription unit *87A7-9/2* and the respective 5′ and 3′ ends of transcription units *87A7-9/1* and *87A7-9/3*.

aur Encodes a Serine-Threonine Protein Kinase

The predicted protein sequence of the *aur* gene is shown in Figure 2. The gene encodes a protein with a predicted molecular mass of 47 kDa, the C-terminal domain of which contains the conserved subdomains of a serine–threonine protein kinase (Hanks et al., 1988). Alignment of this kinase domain with the catalytic domains of other kinases

```
1    MSHPSDHVLRPKENAPHRMPEKSAAVLNMQKNLLLGKKPN
41   SENMAPDSKPLPGSSGALIRSAATTVRPATKPGLGGSNSI
81   ASSEGNNFQKPMVPSVKKTTSEFAAPAPVAPIKKPESLSK
121  QKPTAASSESSKELGAASSSAEKEKTKTETQPQKPKKTWE
161  LNNFDIGRLLGRGKFGNVYLAREKESQFVVALKVLFKRQI
                 I                  II
201  GESNVEHQVRREIEIQSHLRHPHILRLYAYFHDDVRIYLI
                  III                IV
241  LEYAPQGTLFNALQAQPMKRFDERQSATYIQALCSALLYL
                 V
281  HERDIIHRDIKPENLLLGHKGVLKIADFGWSVHEPNSMRM
                 VI                 VII
321  TLCGTVDYLPPEMVQGKPHTKNVDLWSLGVLCFELLVGHA
                VIII                IX
361  PFYSKNYDETYKKILKVDYKLPEHISKAASHLISKLLVLN
                        X                   XI
401  PQHRLPLDQVMVHPWILAHTQ
```

Figure 2. Sequence of the Aur

Overlapping fragments from both strands of cDNA *87A7-9/2* and its corresponding genomic region were sequenced using Sequenase kits (United States Biochemical Corporation). The predicted protein sequence of *aur* is shown. The kinase subdomains are labeled I–XI, and the absolutely conserved amino acids within these domains are underlined and displayed in boldface; other highly conserved residues are shown in boldface. The predicted protein contains 421 amino acids and has a predicted molecular mass of 47.3 kDa and a pI of 9.94.

shows the *aur* kinase most closely resembles the cAMP-dependent protein kinases, showing 38% identity with the kinase domains of the *TPK1* and *TPK3* genes of budding yeast, for example (Toda et al., 1987). However, the 160 amino acid N-terminal extension of the *aur* kinase shows no sequence homology with any of these enzymes. We have determined the sequence of one of the strong mutant alleles, aur^{e209}, and find that this differs from wild type in two positions. It has an asparate to alanine change at residue 47, and the glutamate that is normally absolutely conserved in kinase subdomain III (residue 212) is changed to a lysine residue, consistent with the amorphic nature of this allele.

Embryos Derived from *aur* Females Show an Abnormal Distribution of Centrosomes on Mitotic Spindles

Our initial observations of *aur*-derived embryos stained with Hoechst 33258 showed them to be undergoing asynchronous nuclear divisions during nuclear cycles 10–13 and revealed uneven distributions of nuclei. We sought to examine the arrangements of microtubules and centrosomes in these embryos by immunostaining with antibodies YL1/2, which recognizes tubulin (Kilmartin et al., 1982), and Bx63 or Rb188, which recognizes CP190, which associates with the centrosome during mitosis (Frasch et al., 1986; Whitfield et al., 1988; Kellogg and Alberts, 1992). (CP190 is recognized by monoclonal antibody Bx63 in the nuclei of interphase cells and in association with centrosomes during mitosis [Frasch et al., 1986]. Its gene was cloned by Whitfield et al. [1988]. The antigen has also been termed DMAP190, reflecting its isolation in microtubule preparations [Kellogg and Alberts, 1992]. In agreement with Alberts' laboratory, we now rename the antigen CP190, for 190 kDa centrosome-associated protein, to avoid further confusion.)

One of the earliest mitotic defects to be seen in *aur*-derived embryos are prometaphase nuclei in juxtaposition to paired sets of centrosomes (Figure 3). These paired centrosomes, in many instances, function together as a single pole to nucleate bipolar spindles associated with two groups of condensed chromosomes (see arrows in Figure 3). This is in contrast with wild-type syncytial embryos in which closely separated centrosomes are seen following their duplication at telophase (Huettner, 1933; Karr and Alberts, 1986; Warn and Warn, 1985). The closely paired centrosomes have the appearance of newly duplicated structures, suggesting either that centrosome duplication is occurring at an inappropriate time or that there is a defect in centrosome separation. Such events could lead to the unusual distribution of nuclei in relation to the mitotic spindle either as a consequence of anaphase de-

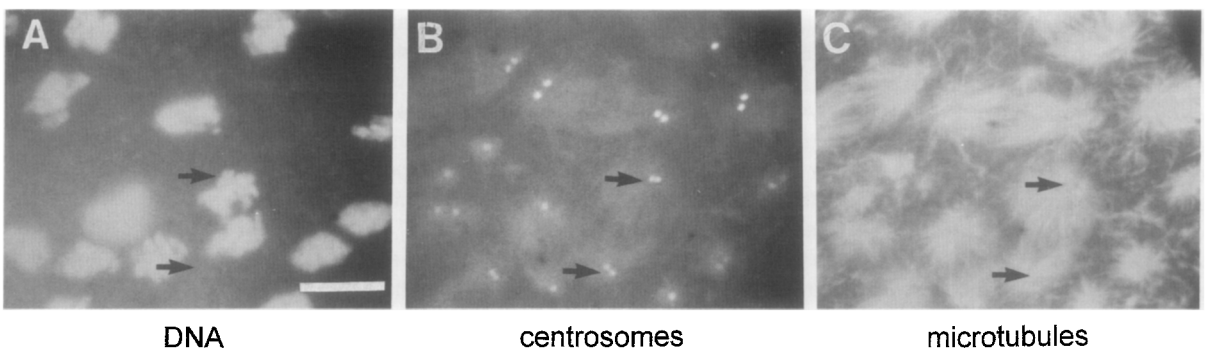

Figure 3. Twinned Centrosomes at Prometaphase in *aur*-Derived Embryos

Embryos derived from mothers homozygous for the $aur^{074\text{-}18}$ allele were prepared for indirect immunofluorescence (see Experimental Procedures) using the rabbit antibody Rb188 (Whitfield et al., 1988) directed against centrosomes (B), the rat monoclonal antibody YL1/2 (Kilmartin et al., 1982) to reveal microtubules (C), and Hoechst to reveal DNA (A) and were examined by conventional fluorescence microscopy on a Zeiss Standard microscope. Many nuclei are associated with two pairs of centrosomes, and several of these are associated with two sets of condensed chromosomes (indicated by arrows). Free centrosomes can also be seen. Scale bar is 10 μm.

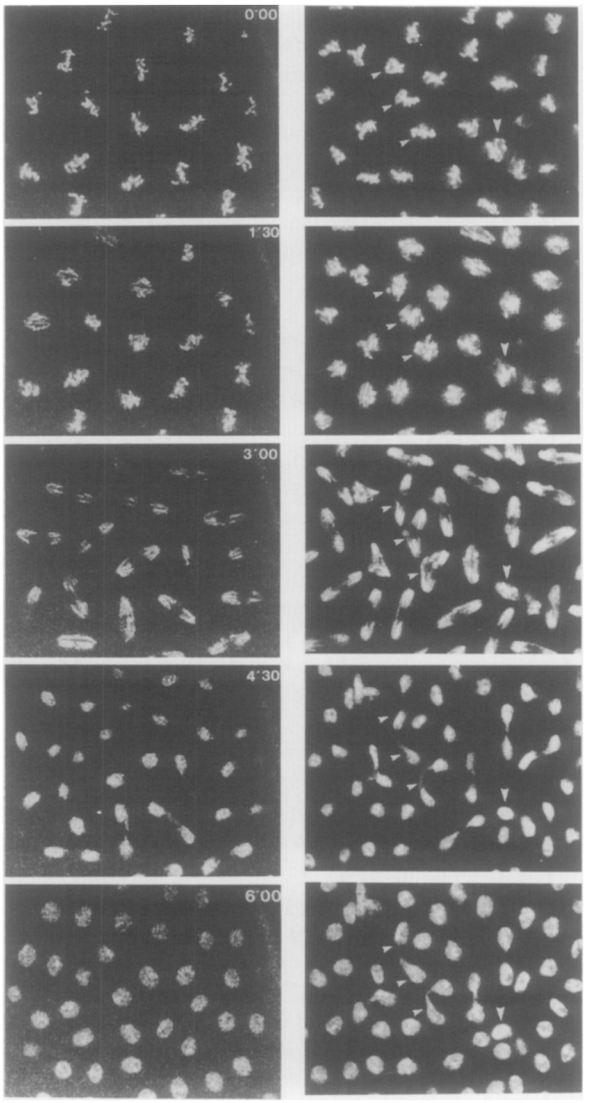

Figure 4. The Progression of Abnormal Mitoses in Real Time in *aur*-Derived Embryos

Embryos derived from either wild-type (left) or homozygous $aur^{074\text{-}18}$ mothers (right) were injected with rhodamine-labeled histones following the protocols of Minden et al. (1989). Confocal images were taken at 30 s intervals (see Experimental Procedures), of which every third image is displayed, showing chromsomes at metaphase (0 time), early anaphase (1.5 min), midanaphase (3 min), early telophase (4.5 min), and late telophase (6 min). The three adjacent nuclei labeled with small arrowheads in the *aur*-derived embryos form interconnected anaphases that do not correctly resolve. The single nucleus labeled with a single larger arrowhead fails to complete anaphase and becomes a tetraploid telophase nucleus.

fects or as a failure of the microtubule-organizing centers to separate at telophase or subsequent stages.

Other embryos show more extreme mitotic defects in which spindle structures associated with discrete groups of condensed chromosomes become intricately branched, sharing common centrosomes as microtubule-organizing centers (data not shown). Free centrosomes that have dissociated from spindles can also be seen in such embryos, as has been also observed with several other Drosophila mitotic mutants (Freeman et al., 1986; Gonzalez et al., 1990; Sullivan et al., 1990; Vessey et al., 1991). Mitotic abnormalities appear to accumulate in these later syncytial cycles, leading to embryos that have many polyploid nuclei.

To ascertain how those multipolar spindle structures observed in fixed preparations might arise, we followed mitosis in real time by injecting *aur*-derived embryos with rhodamine-labeled histone. A comparison of a mitotic cycle in wild-type and mutant embryos is shown in Figure 4. Several mitotic abnormalities can be seen in this field from *aur*-derived embryos, of which two events are highlighted by arrows. In one case, indicated by small arrowheads, three juxtaposed metaphase nuclei (0 time) can be seen to enter anaphase (1.5 min), with some chromatids appearing to be pulled toward the pole of the neighboring spindle (3 min). This results in the formation of chromatin bridges at telophase (4.5 min). The single nucleus marked with the larger arrowhead appears to enter an anaphase (1.5 min) that is never completed. Its chromosomes regress and then decondense at telophase in the former position of the metaphase plate. The resulting interphase nucleus appears tetraploid by the increased intensity of its fluorescence relative to neighboring nuclei. These defects appear similar to those described by Sullivan et al. (1990) for *daughterless abnormal oocyte like* (*dal*)-derived embryos in which abnormal centrosome separation appears to take place.

Brains of Larval Lethal Alleles of *aur* Show an Elevated Mitotic Index and Circular Mitotic Figures

Although the phenotypes shown by the embryos of *aur* mothers point toward a defect in centrosome behavior, many mitotic mutants (Freeman et al., 1986; Gonzalez et al., 1990; Sullivan et al., 1990; Vessey et al., 1991) and drug treatments (Raff and Glover, 1988) can have secondary consequences upon centrosomes that are difficult to distinguish from primary defects. Moreover, the female sterile alleles of *aur* are hypomorphic, whereas amorphic alleles lead to larval lethality. We therefore examined the effects of various combinations of mutant *aur* alleles upon mitosis in neuroblasts of the larval brain. Such cells are subject to checkpont controls that monitor the progression through the mitotic cycle, and so mitotic defects can block cell cycle progression. We were unable to find mitotic defects in squashed preparations of the brains of homozygous $aur^{287\text{-}19}$ larvae, but saw only figures with wild-type appearance (data not shown). The zygotically produced mutant protein must therefore be sufficient, together with perduring maternal wild-type protein for normal mitosis. When the dose of mutant protein is reduced in $aur^{287\text{-}19}$/*Df(3R)T-61* larvae, however, there are a low but significant number of abnormal mitotic figures. The brains from such larvae contain several polyploid figures (Figure 5A), but the mitotic index and the ratio of anaphases to metaphases are otherwise normal. A more dramatic phenotype is seen in heterozygous aur^{e170}/aur^{e209} larvae, which have very few

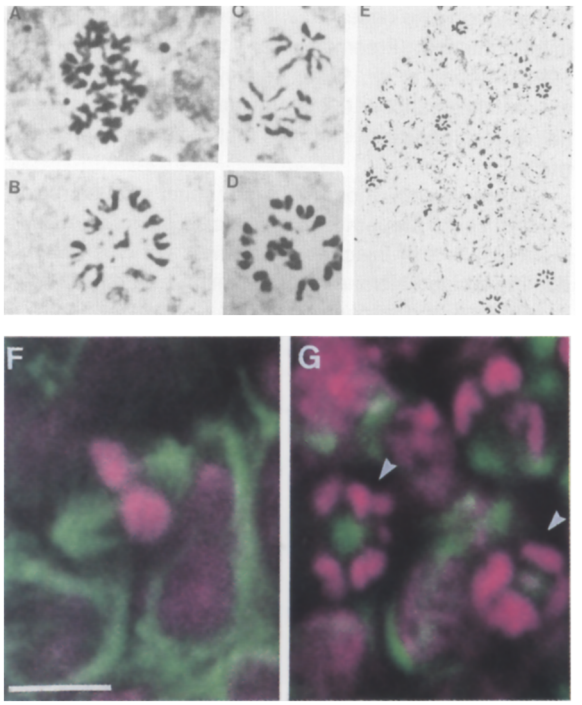

Figure 5. Squashed and Whole-Mount Preparations of *aur* Brains

Brains of third instar larvae were prepared as described in Experimental Procedures.

(A) A polyploid metaphase figure from an $aur^{287}/Df(3R)T\text{-}61$ larva.

(B) A circular polyploid figure from an aur^{e170}/aur^{e209} larva.

(C) An anaphase figure from an $aur^{e170}/Df(3R)KarD^{1}$ larva. Note that the chromosomes at both poles appear to be arranged in a circular configuration.

(D) A CMF from a $Df(3R)KarD^{1}/Df(3R)T\text{-}61$ larva.

(E) A low magnification view of a field of cells from a $Df(3R)KarD^{1}/Df(3R)T\text{-}61$ larva, showing seven CMFs.

(F) A bipolar spindle from a wild-type brain in which chromosomes stained with propidium iodide are shown in purple and spindle microtubules, revealed using antibody YL1/2, are shown in green.

(G) CMFs (indicated by arrowheads) from an $aur^{e209}/Df(3R)T\text{-}47$ larval brain.

Scale bar for (F) and (G) is 10 μm.

normal metaphase and anaphase figures, and many circular mitotic figures (CMFs) (Figure 5B). These comprise circular chromosomal arrangements in which the major autosomes and sex chromosomes lie on the periphery of the circle, with their centromeres pointing inward and their telomeres pointing outward. The small fourth chromosomes are located in the center of these circles. The arrangement of chromosomes is strikingly similar to that described by Gonzalez et al. (1988) for mutations in *mgr*. As with *mgr*, the chromosomes appear to be attached to microtubules and under traction in that when larval brains are treated with colchicine to destabilize microtubules, circular metaphase figures are no longer seen. Over either of the deficiencies, *Df(3R)T-61* or *Df(3R)KarD*^{1}, aur^{e209} shows a larval neuroblast phenotype exactly like that of aur^{e170}/aur^{e209} larvae (data not shown). aur^{e170} cannot be examined over both of these deficiencies since it carries an additional early lethal mutation in the interval uncovered by *Df(3R)T-61* (see Experimental Procedures). However, over *Df(3R)KarD*^{1}, it shows this same phenotype of circular metaphase-like configurations, together with anaphase figures in which chromosomes appear to be arranged in circles around each of the poles (Figure 5C). Larvae that are heterozygous for these overlapping deficiencies and that are therefore entirely deficient for the 87A8-9 interval also die as pupae and have the same neuroblast phenotype as the lethal allele/deficiency heterozygotes, confirming the amorphic nature of these lethal alleles (Figures 5D and 5E).

Circular Figures Are Arranged on Monopolar Spindles around Large Centrosomes

Gonzalez et al. (1988) have proposed that the CMFs observed in *mgr* are monopolar spindles. To determine whether this is the case in *aur* neuroblasts, we utilized confocal microscopy to examine the structure of the mitotic apparatus in whole-mount preparations of third instar larval brains. A normal bipolar spindle in metaphase is shown in Figure 5F. Mutant figures, displayed in Figure 5G (arrowheads), show large astral-like arrays of microtubules emanating from single organizing centers and having chromosomes arranged in a circular configuration similar to the arrangement seen in squashed orcein-stained preparations.

To examine the localization of centrosomes in such structures, we carried out immunostaining with antibodies to the CP190 protein. Single fields of cells from brains with several different allelic combinations of *aur* showed multiple mitotic figures, in which only a single centrosome could be found by optical sectioning (e.g., cells indicated by arrowheads in Figure 6A). The radial arrays of microtubules emanating from the single centrosomal structures in individual cells from aur^{e200}/aur^{e209} brains can be seen in Figure 6B. Measurement of the maximal width of these centrosomal structures showed them to be larger than the centrosomes at the poles of bipolar spindles (Figure 6C), consistent with them being an aggregate of two recently duplicated centrosomes. Indeed, although the majority of monopolar spindles contained a single immunostained structure (Figure 6D), closely separated pairs of centrosomes could be seen in some cells (Figure 6E). These are scored as two individual (small) centrosomes in the histogram shown in Figure 6. In several respects, these resemble the duplicated centrosomes that can be seen in *aur* embryos (see Figure 3). Thus, it appears that centrosomes have at least partially duplicated in *aur* neuroblasts, but failed to separate, resulting in the failure to establish a bipolar spindle.

Discussion

Chromosome Organization at 87A7-9

In the course of this work, we have physically mapped 42–45 kb of DNA to an interval that includes only the extremely thin band A8 and part of the moderately thick band A9 between the *Df(3R)KarD*^{1} and *Df(3R)T-61* deficiency breakpoints. This agrees well with the correlations made by Spierer et al. (1983) between polytene band density and DNA content. However, the number of transcription

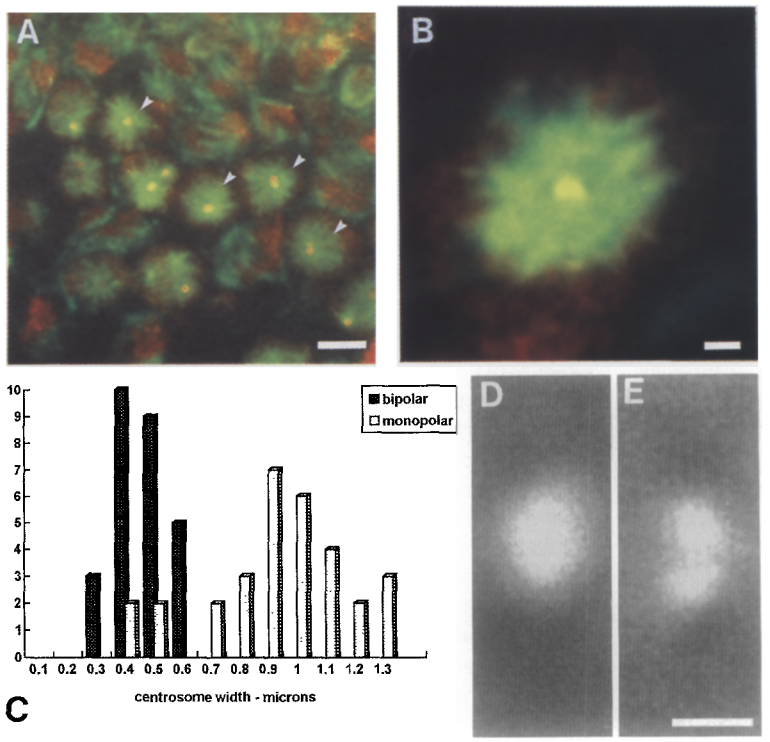

Figure 6. Centrosome Organization in *aur* Brains

(A) A field of cells from the brain of an aur^{e200}/aur^{e209} larva. At least four monopolar mitotic cells (indicated by arrowheads) have single centrosomes in the center of a radial array of microtubules. The mitotic centrosome (yellow) is revealed by the rabbit antibody Rb188 directed against the Bx63 centrosome-associated antigen (Whitfield et al., 1988). Microtubules (green) are revealed using the rat monoclonal antibody YL1/2 (Kilmartin et al., 1982). Scale bar is 10 μm.

(B) Single (duplicated and slightly separated) centrosome in the center of a radial array of microtubules in a mitotic cell from an aur^{e200}/aur^{e209} larval brain. Scale bar is 1 μm.

(C) Histogram comparing centrosome width in wild-type bipolar mitotic spindles (immunostaining not shown) and monopolar spindles from aur^{e200}/aur^{e209} and aur^{e200}/aur^{e170} brains. The centrosomes of wild-type width within the monpolar structures were invariably paired (see [E]).

(D) Duplicated centrosome within a monpolar structure from an aur^{e200}/aur^{e209} larva.

(E) Slightly separated centrosomes in a monopolar structure from an aur^{e200}/aur^{e170} cell. Scale bar for (D) and (E) is 1 μm.

units in this interval is greater than anticipated. In a previous study using Northern blots on total embryonic RNA, Udvardy et al. (1985) were able to detect only one transcription unit within the 11 kb genomic interval that extends distally from *hsp70*. We have isolated cDNAs corresponding to four transcription units within this interval. The 3′ of transcription unit *87A7-9/1* either overlaps or is extremely close to that of *hsp70*, and its 5′ end is separated from the 5′ end of transcription unit *87A7-9/2* (*aur*) by approximately 250 bp. This region of common upstream sequence corresponds exactly to a region to which Udvardy and colleagues have mapped a specific chromatin structure (scs′) (Udvardy et al., 1985; Farkas and Udvardy, 1992). The scs′ consists of two strong nuclease hypersensitive sites separated by a nuclease-resistant core and has been postulated to be a boundary structure serving as a functional barrier to insulate *hsp70* gene enhancers (Farkas and Udvardy, 1992) and to be a focal point for the decondensation of the A7 chromomere when the *hsp70* gene is activated during heat shock (Udvardy et al., 1985; see also Lewin, 1994). While this could also be a function for this DNA, it is likely to contain important regulatory sequences for two divergent and previously unrecognized transcription units and can be seen as a nuclease-protected region in the assays reported by Udvardy et al. (1985). These and one other nuclease-protected region correspond exactly with the positions of cDNAs *87A7-9/1*, *87A7-9/2*, and *87A7-9/3*. In total, we detect at least eight transcription units within the 42–45 kb 87A8-9 interval. However, in a lethal saturation screen, Gausz et al. (1981) were only able to isolate one lethal complementation group (ck^{19}) within this cytological interval. We have shown that this complementation group corresponds to the *aur* locus. The frequency with which lethal complementation groups were recovered does suggest that this screen approaches saturation, which indicates that as many as seven of the eight transcription units at 87A8-9 may be unnecessary for the survival of Drosophila in laboratory conditions.

aur Affects Centrosome Behavior: Effects of Different Mutant Alleles

Flies homozygous for weaker hypomorphic alleles of *aur* can survive until adulthood. However, the rigorous demands of the rapid rounds of syncytial mitoses are not met in embryos derived from *aur* mothers. Several of the abnormalities that are seen within these embryos, including asynchronous nuclear divisions, the dissociation of centrosomes, and the generation of polyploid nuclei, can also be seen in other mitotic mutants showing a maternal effect. It is particularly common to see centrosomes dissociate from nuclei and appear to undergo autonomous replication cycles, first seen in *gnu*-derived embryos (Freeman et al., 1986), but also seen following the inhibition of DNA synthesis with aphidicolin (Raff and Glover, 1988), indicating that these syncytial cycles lack some of the checkpoint controls that coordinate mitotic events. It is therefore likely that some aspects of the phenotype of *aur*-derived embryos are not directly related to the primary defect, but are instead multiple consequences of mutations that disrupt the cell cycle. This is likely to be exacerbated by the leaky nature of these alleles. Nevertheless, the mitotic apparatus of *aur*-derived embryos has some characteristic features that give insight into the primary role of the *aur* kinase. In addition to bipolar spindles with a centrosome at each pole, there are monopolar spindles associated with either one or two very closely paired or associated

centrosomes, with bipolar spindles with two very closely paired centrosomes at each pole, and with complexed spindles with shared centrosomes at some poles. Complex spindles of this type have been observed to arise in *dal*-derived embryos when the centrosome associated with one nucleus fails to separate and its astral microtubules then link to the adjacent spindle (Sullivan et al., 1990). Our observations of *aur*-derived embryos would be consistent with a similar mechanism. Paired centrosomes are normally seen in wild-type embryos at telophase when the centrosome duplicates in preparation for the next mitotic cycle. This feature of *aur*-derived embryos can explain many of the mitotic abnormalities that subsequently arise in the syncytial cycles. While the embryonic phenotype of the weak *aur* alleles points toward a defect in the centrosome cycle, a clear indication of abnormal centrosome behavior is seen in neuroblasts from larvae carrying amorphic alleles, a high proportion of which have monopolar spindles.

Monopolar Spindles

Monopolar spindles have been previously described in organisms other than Drosophila, either occurring as intermediates in normal mitoses or resulting from mutation or drug treatment. The classical experiments of Mazia et al. (1960) showed that when sea urchin eggs were treated with mercaptoethanol at metaphase, they would divide into four cells, each of which would assemble a monopolar spindle during the next mitosis. It was proposed that each spindle pole contained two polar organizers that became split without duplication, giving rise to poles with only half the normal reproductive capacity. This has been found to correlate with the number of centriole pairs, poles with half the reproductive capacity, having only one centriole (Sluder and Begg, 1985; Sluder and Rieder, 1985).

It appears from the size of the centrosomes, which nucleate monopolar spindles in *aur* cells, that rather than being split, they have at least partially duplicated and that centrosome separation has not occurred. However, it remains important to address this question at the ultrastructural level since it is possible either that the defect in *aur* is in the process of centrosomes separation per se or that centrosomes fail to separate because the duplication process is incomplete. Electron microscopical analysis of centrosomes in the *aur* mutants and in wild-type cells is in progress.

Wang et al. (1983) have also suggested that the defect in a temperature-sensitive mutant Syrian hamster cell line also results in a failure of centrosome separation. At the nonpermissive temperature, these cells also develop monopolar spindles in which chromosomes adopt a circular configuration. They proceed through through several cell cycles to become polyploid. Monopolar structures also arise naturally during mitosis in vertebrate cells, either when the replicated centrosomes do not separate before nuclear envelope breakdown or if they migrate too far apart for the asters to make contact and establish a bipolar spindle. This has been extensively studied in newt lung cells (Bajer, 1982; Waters et al., 1993). Chromosomes become attached and are pulled to these monopoles by a single kinetochore fiber, although the arms are pushed away from the pole (Cassimeris et al., 1994), an arrangement exactly as seen in *aur* cells.

Toward Understanding the Centrosome Duplication-Separation Cycle

The phenotype of *dal*-derived embryos suggests that this gene also has a role in centrosome separation (Sullivan et al., 1990). However, only a single mutant allele of *dal* has been described, and in the absence of amorphic alleles, it is difficult to assess the phenotype fully. The formation of monopolar spindles in larval neuroblasts has now been described in strong mutant alleles of several different loci in Drosophila. The monopolar structures seen in *aur* brains are quite distinct from those resulting from mutations in *asp*, in which a single centrosome can be seen to nucleate what is best described as a "hemispindle" in which asymmetric arrays of microtubules emanate from a centrosome close to the plasma membrane of the cell toward clustered condensed chromosomes not in a circular configuration (Ripoll et al., 1985; Gonzalez et al., 1990). The circular arrangements of mitotic figures in squashed preparations of *aur* brains closely resembles those described by Gonzalez et al. (1988) for the mitotic mutant *mgr*, the gene for which has not yet been cloned. The similarity with the *aur* phenotype extends to the fact that the centrosome at the center of the *mgr* monoastral spindle is approximately twice the width of centrosomes at the poles of bipolar spindles, again suggesting a failure of centrosome separation after at least partial duplication (C. Gonzalez, unpublished data). Heck et al. (1993) have described a mutation in a gene encoding a kinesin-like protein at 61F that results in the formation of monopolar spindles in larval neuroblasts. It seems likely that in the *KLP61F* mutant, a monopolar spindle is formed through a failure of this motor to mediate the separation of centrosomes and so establish a bipolar spindle.

Waters et al. (1993) have studied centrosome separation in newt cells during prophase/prometaphase and in the so-called anaphase-like metaphase, when asters associated with widely separated centrosomes fail to connect and form a bipolar spindle. The kinetics of centrosome separation appear identical whether or not the microtubule arrays overlap, suggesting that each centrosome generates its own intrinsic force. Such a force could be provided by a kinesin-like protein such as that encoded in Drosophila by *KLP61F*. As with most kinases, it will be difficult to determine the substrates of the *aur* enzyme. Indeed, a number of phosphoproteins are known to be associated with spindle poles at the onset of mitosis (Vandre et al., 1984, 1986), together with a number of kinases, including cAMP-dependent kinase II (Nigg et al., 1985; Keryer et al., 1990) and $p34^{cdc2}$ (e.g., Bailly et al., 1989). However, the finding that mutations in *mgr* and *KLP61F* have such similar phenotypes suggests that they have a role in a common process, and it will be of future interest to determine whether the *aur* kinase can phosphorylate their gene products and thereby regulate their function.

Experimental Procedures

Complementation between Chromosomes Carrying ck^{10} Alleles

The results of complementation tests are shown in Table 1. The ck^{10} complementation group is uncovered by *Df(3R)KarD*^{1} and *Df(3R)T-61*, resulting in pupal lethality or female sterility. Each of the ck^{10} chromosomes carry additional mutations, some of which map in the 86E3-6–87D1-2 region. The e^{209} and e^{200} chromosomes each carry additional third instar lethals outside the interval; the e^{170} chromosome has an additional embryonic lethal that is uncovered by *Df(3R)T-61* but not *Df(3R)KarD*^{1}; the e^{160} chromosome has a weak hypomorphic allele of the ck^{10} complementation group and pupal lethal mutation that maps between 87A9 and 87D1-2; and the hs^{65} chromosome has an additional embryonic lethal that maps between 87A9 and 87D1. The double deficiency heterozygote *Df(3R)KarD*^{1}*/Df(3R)T-61* also dies at the pupal stage. The mutation aur^{287} leads to female sterility when aur^{287} is placed against all of the ck^{10} alleles, indicating that the *aur* and ck^{10} alleles are representatives of the same complementation group.

Walk from the Proximal Breakpoint of *Df(3R)KarD*^{1} to the Distal Breakpoint of *Df(3R)T-61*

This chromosomal walk was initiated from the distal genomic sequences contained within the plasmids CHS-8 and CHS-Sal, which overlap extensively and extend 15 kb from *hsp70*. An end fragment of the CHS-8 insert was used to probe a genomic DNA library in the λDASH vector. One positive fragment (λSal) contained an 18 kb insert that extended the walk by 12.5 kb. Subsequent steps used probes synthesized from the λDASH vector, using T7 and T3 RNA polymerases for counterscreening. Two phage isolated in this way, φ11 and φ8, extended the walk by 9.3 kb and 16 kb, respectively. To determine whether the walk had reached the distal breakpoint of *Df(3R)T-61*, Southern blot experiments were performed on DNA from wild-type (Oregon R) and *Df(3R)T-61/+* flies probed with phage DNA or subcloned segments of the phage inserts. Probes from CHS-Sal, CHS-8, λSal, and φ11 detected no differences in the restriction patterns of wild-type and *Df(3R)T-61/+* DNA (data not shown), whereas the φ8 probe detected novel bands of hybridization. By this criterion, a 13 kb SalI fragment was found to be unique to the *Df(3R)T-61* chromosome. This genomic fragment was cloned, its restriction endonuclease cleavage sites mapped, and the breakpoint positioned within a 2.2 kb SalI–HindIII fragment. In situ hybridization experiments with the cloned 13 kb SalI fragment showed it to contain sequences present at 87A9 and 86E3-6 on wild-type polytene chromosomes (Figure 1). The localization of this breakpoint at 86E3-6 is in agreement with cytologial mapping carried out by C. Gonzalez (personal communication) and is at variance with the published cytology (Gausz et al., 1981).

cDNAs Corresponding to Genes within the 87A8-9 Interval

Eight cDNAs were isolated using probes prepared from fragments of genomic DNA from between the *Df(3R)T-61* and *Df(3R)KarD*^{1} breakpoints. Each cDNA was positioned by Southern blot hybridization to digests of cloned genomic DNA and by restriction endonuclease cleavage mapping. cDNA1 was found to have an EcoRI site 100 bp from its 5′ end, and cDNA2 was found to have a BamHI site 150 bp from its 5′ end. As these cleavage sites are separated by 500 bp on the genome, this suggests that the 5′ ends of these cDNAs are separated by 250 bp. The 3′ end of cDNA1 probably overlaps with the 3′ end of the distal-most *hsp70* gene by 100 bp, because it is 2.0 kb in length, and its 5′ end is 1.9 kb from the 3′ end of this *hsp* gene.

Mapping *aur* within 87A8-9 by P Element–Mediated Transformation

Construct I, which carries transcription unit *87A7-9/6* , is the 15.4 kb SalI insert of λSal inserted into pW8 that had been digested with XhoI. This segment of genomic DNA has a 2.5 kb deletion in the aur^{e170} chromosome. The construct is unable to rescue the sterility of $aur^{287\text{-}19}$, indicating the deletion has no relationship with *aur*. Construct II, which carries transcription units *87A7-9/1* to *87A7-9/5* and is able to rescue the sterility of $aur^{287\text{-}19}$, was made by ligating the 16.2kb SalI fragment of CHS-Sal to XhoI-digested pW8. Construct III fails to rescue, thus eliminating transcription units *87A7-9/4* and *87A7-9/5* as *aur* candidates. It was made by ligating the 13.7 kb EcoRI frgament of CHS-8 to pW8 digested with EcoRI. A further construct was made (construct IV) by inserting a 7 kb XbaI–SalI fragment of CHS-Sal to XhoI–XbaI-digested pW8, but it was not used for transformation. Construct V, which rescues and which contains the intact transcription units *87A7-9/1* to *87A7-9/3*, comprises the 9 kb XbaI–SalI fragment of CHS-Sal ligated to XbaI–XhoI-digested pW8. Construct VI, which carries transcription unit *87A7-9/3* and is unable to rescue, was made by ligating the 6.5 kb NcoI fragment of CHS-Sal to HpaI-digested pW8. Construct VII, which fails to rescue, is the 6 kb EcoRI–HindIII fragment of CHS-8, carrying transcription unit *87A7-9/4* ligated to HpaI-digested pW8. Construct VIII, which carries the intact region corresponding to cDNA *87A7-9/2*, is a 3.7 kb EcoRI fragment from CHS-Sal, which rescues $aur^{287\text{-}19}$, thus defining the gene.

The initial set of transformants were made by coinjecting the pW8 construct into w^{1118} embryos with helper plasmid. Subsequently, the line constructed by Robertson et al. (1988), which carries a single stable insert of PΔ2-3 at 99B, was used as a host in transformation experiments. Adult survivors were individually crossed to w^{1118} flies, and their progeny (G1) were screened for the presence of flies with red-orange eyes, from which stocks were established. To test rescue of $aur^{ts(3)}$ alleles, we crossed transformed lines to balanced $aur^{287\text{-}19}$/*TM3* flies in a w^{1118} background. Progeny that were w^{+} and carried the *TM3* balancer were again crossed to $aur^{287\text{-}19}$/*TM3* flies in a w^{1118} background. Male and female progeny that were $aur^{287\text{-}19}$/*TM3* P[w^{+}] were selected and self-crossed. As the *aur* chromosome carries *ru st e ca*, homozygous females were recognized by these markers and tested for sterility. Chromosomes carrying lethal alleles aur^{e170} and aur^{e209} were then introduced into such lines, and the viability of such heterozygotes was monitored.

Cytological Analyses

Immunostaining of embryos, whole-mount preparations of larval brains, and preparation and examination of squashed larval brains were all carried out as described by Gonzalez and Glover (1993).

Acknowledgments

Correspondence should be addressed to D. M. G. This study was initiated during a visit by D. M. G. to Tübingen, Federal Republic of Germany, as a short-term European Molecular Biology Organization fellow in 1985. We wish to thank Christiane Nüsslein-Volhard for providing the *aur* alleles and for her encouragement in the early stages of this project. We wish to thank Janos Gausz (Szeged) for his gift of ck^{10} alleles and Andor Udvardy (Szeged) for his gift of cloned DNAs extending distally from 87A7. Cayetano Gonzalez provided assistance with the cytology of the 86/87 region and gave helpful advice throughout this project. Luke Alphey and Fiona Cullen kindly helped with DNA sequencing, and Will Whitfield helped with the real-time observations of mitosis following the injection of tagged histones into syncytial embryos. Part of this work, carried out in the Department of Biochemistry at Imperial College, was submitted by M. H. L. for his Ph.D. degree at the University of London in 1990. The body of the work has been supported by the Cancer Research Campaign, and we are also grateful to the Medical Research Council for a training fellowship to H. P. and for a research studentship to D. A. M.

Received July 13, 1994; revised February 5, 1995.

References

Bailly, E., Dorée, M., Nurse, P., and Bornens, M. (1989). p34^{cdc2} is located in both nucleus and cytoplasm: part is centrosomally associated at G2/M and enters vesicles at anaphase. EMBO J. *8*, 3985–3995.

Bajer, A. S. (1982). Functional autonomy of monopolar spindle and evidence for oscillatory movement in mitosis. J. Cell Biol. *93*, 33–48.

Brown, N. H., and Kafatos, F. C. (1988). Functional cDNA libraries from *Drosophila* embryos. J. Mol. Biol. *203*, 425–437.

Caggese, C., Caizzi, R., Morea, M., Scalenghe, F., and Ritossa, F. (1979). Mutation generating a fragment of the major heat-shock induc-

ible polypeptide in *Drosophila melanogaster*. Proc. Natl. Acad. Sci. USA *76*, 2385–2389.

Callaini, G., and Riparbelli, M. G. (1990). Centriole and centrosome cycle in early *Drosophila* embryo. J. Cell Sci. *97*, 539–543.

Cassimeris, L., Reider, C. L., and Salmon, E. D. (1994). Microtubule assembly and kinetochore directional instability in vertebrate monopolar spindles: implications for the mechanism of chromosome congression. J. Cell Sci. *107*, 285–297.

Farkas, G., and Udvardy, A. (1992). Sequence of scs and scs' *Drosophila* DNA fragments with boundary function in the control of gene expression. Nucl. Acids Res. *20*, 2604.

Fenton, B., and Glover, D. M. (1993). *polo*, a conserved mitotic kinase, is active at late anaphase–telophase in the syncytial *Drosophila* embryo. Nature *363*, 637–639.

Frasch, M., Glover, D. M., and Saumweber, H. (1986). Nuclear antigens follow different pathways into daughter nuclei during mitosis in early *Drosophila* embryos. J. Cell Sci. *82*, 155–172.

Freeman, M., Nüsslein-Volhard, C., and Glover, D. M. (1986). The dissociation of nuclear and centrosomal division in *gnu*, a nuclear replication mutant of Drosophila. Cell *46*, 457–468.

Gard, D. L., Hafezi, S., Zhang, T., and Doxsey, S. J. (1990). Centrosome duplication continues in cycloheximide-treated *Xenopus* blastulae in the absence of a detectable cell cycle. J. Cell Biol. *110*, 2033–2042.

Gatti, M., and Baker, B. S. (1989). Genes controlling essential cell cycle functions in *Drosophila melanogaster*. Genes Dev. *3*, 438–453.

Gausz, J., Gyurkovics, H., Bencze, G., Awad, A. A. M., Holden, J. J., and Ish-Horowicz, D. (1981). Genetic characterization of the region between 86F1,2 and 87B15 on chromosome 3 of *Drosophila melanogaster*. Genetics *98*, 775–789.

Girdham, C., and Glover, D. M. (1991). Chromosome tangling and breakage at anaphase result from mutations in *lodestar*, a *Drosophila* gene encoding a putative nucleoside triphosphate binding protein. Genes Dev. *5*, 1786–1799.

Gonzalez, C., and Glover, D. M. (1993). Techniques for studying mitosis in *Drosophila*. In The Cell Cycle: A Practical Approach, P. Fantes and R. Brooks (Oxford: IRL Press), pp. 163–168.

Gonzalez, C., Casal, C., and Ripoll, P. (1988). Functional monopolar spindles caused by mutation in *mgr*, a cell division gene of *Drosophila melanogaster*. J. Cell Sci. *89*, 39–47.

Gonzalez, C., Saunders, R., Casal, J., Molina, I., Carmena, M., Ripoll, P., and Glover, D. M. (1990). Mutations at the *asp* locus of *Drosophila* lead to multiple free centrosomes in syncytial embryos, but restrict centrosome duplication in larval neuroblasts. J. Cell Sci. *96*, 605–616.

Hanks, S. K., Quinn, A. M., and Hunter, T. (1988). The protein kinase family: conserved features and deduced phylogeny of the catalytic domains. Science *241*, 42–52.

Heck, M. M. S., Pereira, A., Pesavento, P., Yannoii, Y., Spradling, A. C., and Goldstein, L. S. B. (1993). The kinesin-like protein KLP61F is essential for mitosis in *Drosophila*. J. Cell Biol. *123*, 665–679.

Huettner, A. F. (1933). Continuity of the centrioles in *Drosophila melanogaster*. Z. Zellforsch. Mikrosk. Anat. *19*, 119–134.

Ish-Horowicz, D., and Pinchin, S. M. (1980). Genomic organisation of the 87A7 and 87C1 heat-induced loci of *Drosophila melanogaster*. J. Mol. Biol. *142*, 231–245.

Ish-Horowicz, D., Pinchin, S. M., Gausz, J., Gyurkovics, H., Bencze, G., Goldschmidt-Clermont, M., and Holden, J. J. (1979). Deletion mapping of two D. melanogaster loci that code for the 70,000 Dalton heat-induced protein. Cell *17*, 565–571.

Karr, T. L., and Alberts, B. M. (1986). Organization of the cytoskeleton in early *Drosophila* embryos. J. Cell Biol. *102*, 1494–1509.

Kellogg, D. R., and Alberts, B. M. (1992). Purification of a multiprotein complex containing centrosomal proteins from the *Drosophila* embryo by chromatography with low-afffinity polyclonal antibodies. Mol. Biol. Cell. *3*, 1–11.

Keryer, G., Iftode, F., and Bornens, M. (1990). Identification of proteins associated with microtubule-organising centers and filaments in the oral apparatus in the ciliate *Paramecium tetraurelia*. J. Cell Sci. *97*, 553–563.

Kilmartin, J. V., Wright, B., and Milstein, C. (1982). Rat monoclonal antitubulin antibodies derived by using a new non-secreting rat cell line. J. Cell Biol. *93*, 576–582.

Lewin, B. (1994). Genes V (Oxford: Oxford University Press).

Lindsley, D. L., and Zimm, G. G. (1992). The Genome of *Drosophila melanogaster* (San Diego, California: Academic Press).

Llamazares, S., Moreira, M. A., Tavares, A., Girdham, C., Gonzalez, C., Karess, R. E., Glover, D. M., and Sunkel, C. E. (1991). *polo* encodes a protein kinase homologue required for mitosis in *Drosophila*. Genes Dev. *5*, 2153–2164.

Mazia, D., Harris, P. J., and Bibring, T. (1960). The multiplicity of the mitotic centers and the time-course of their duplication and separation. Biophys. Biochem. Cytol. *7*, 1–20.

Minden, J. S., Agard, D. A., Sedat, J. W., and Alberts, B. M. (1989). Direct cell lineage analysis in *Drosophila melanogaster* by time-lapse, three-dimensional optical microscopy of living embryos. J. Cell Biol. *109*, 505–516.

Nagano, H., Hirai, S., Okano, K., and Ikegami, S. (1981). Achromosomal cleavage of fertilised starfish embryos in the presence of aphidicolin. Dev. Biol. *85*, 409–415.

Nigg, E. A., Schäfer, G., Hilz, H., and Eppenberger, H. M. (1985). Cyclic-AMP-dependent protein kinase type II is associated with the Golgi complex and with centrosomes. Cell *41*, 1039–1051.

Nurse, P. (1990). Universal control mechanism regulating onset of M-phase. Nature *344*, 503–508.

Picard, A., Harricane, M.-C., Labbé, J.-C., and Dorée, M. (1988). Germinal vesicle components are not required for the cell cycle oscillator of the early starfish embryo. Dev. Biol. *128*, 121–128.

Raff, J., and Glover, D. M. (1988). Nuclear and cytoplasmic mitotic cycles continue in *Drosophila* embryos in which DNA synthesis is inhibited with aphidicolin. J. Cell Biol. *107*, 2009–2019.

Ripoll, P., Piminelli, S., Valdivia, M. M., and Avila, J. (1985). A cell division mutant of Drosophila with a functionally abnormal spindle. Cell *41*, 907–912.

Robertson, H. M., Preston, C. R., Phillis, R. W., Johnson-Schlitz, D. M., Benz, W. K., and Engels, W. R. (1988). A stable genomic source of P element transposase in *Drosophila melanogaster*. Genetics *118*, 461–470.

Sluder, G., and Begg, D. A. (1985). Experimental analysis of the reproduction of spindle poles. J. Cell Sci. *76*, 35–51.

Sluder, G., and Lewis, K. (1986). Centrosome doubling does not require nuclear–DNA synthesis. Biol. Bull. *170*, 538.

Sluder, G., and Rieder, C. L. (1985). Experimental separation of pronuclei in fertilised sea-urchin eggs: chromosomes do not organise a spindle in the absence of centrosomes. J. Cell Biol. *100*, 897–903.

Sluder, G., Millar, F. J., Cole, R., and Rieder, C. L. (1990). Protein synthesis and the cell cycle: centrosome reproduction in sea urchin eggs is not under translational control. J. Cell Biol. *110*, 2025–2032.

Spierer, P., Spierer, A., Bender, W., and Hogness, D. S. (1983). Molecular mapping of genetic and chromomeric units in *Drosophila melanogaster*. J. Mol. Biol. *168*, 35–50.

Sullivan, W., Minden, J. S., and Alberts, B. M. (1990). *daughterless-abo-like*, a *Drosophila* maternal effect mutation that exhibits abnormal centrosome separation during the late blastoderm divisions. Development *110*, 311–323.

Sunkel, C., and Glover, D. M. (1988). *polo*: a mitotic mutant of *Drosophila* displaying abnormal spindle poles. J. Cell Sci. *89*, 25–38.

Szabad, J., and Bryant, P. J. (1982). The mode of action of *discless* mutations in *Drosophila melanogaster*. Dev. Biol. *93*, 240–256.

Tearle R., and Nüsslein-Volhard, C. (1987). Tübingen mutants and stocklist. Dros. Inf. Ser. *66*, 209–226.

Toda, T., Cameron, S., Saas, P., Zoller, M., and Wigler, M (1987). Three different genes in S. cerevisiae encode the catalytic subunits of the cAMP-dependent protein kinase. Cell *50*, 277–287.

Udvardy, A., Maine, E., and Schedl, P. (1985). The 87A7 chromomere: identification of novel chromatin structures flanking the heat shock locus that may define the boundaries of higher order domains. J. Mol. Biol. *185*, 341–358.

Vandre, D. D., and Borisy, G. G. (1989). Anaphase onset and dephosphorlylation of mitotic phosphoproteins occur concomitantly. J. Cell Sci. *94*, 245–258.

Vandre, D. D., Davis, F. M., Rao, P. N., and Borisy, G. G. (1984). Phosphoproteins are components of mitotic microtubule organization centers. Proc. Natl. Acad. Sci. USA *81*, 4439–4443.

Vandre, D. D., Davis, F. M., Rao, P. T., and Borisy, G. G. (1986). Distribution of cytoskeletal proteins sharing a conserved phosphorylated epitope. Eur. J. Cell Biol. *41*, 72–81.

Verde, F., Labbé, J.-C., Dorée, M., and Karsenti, E. (1990). Regulation of microtubule dynamics by cdc2 protein kinase in cell free extracts of *Xenopus* eggs. Nature *343*, 233–238.

Vessey, K. B., Ludwiczak, R. L., Briot, A. S., and Underwood, E. M. (1991). *abnormal-chromatin* (*abc*), a maternal-effect locus in *Drosophila melanogaster*. J. Cell Sci. *98*, 233–243.

Wang, R. J., Wissinger, W., King, E., and Wang, G. (1983). Studies on cell division in mammalian cells. VII. A temperature-sensitive cell line abnormal in centriole separation and chromosome movement. J. Cell Biol. *96*, 301–306.

Warn, R. M., and Warn, A. (1985). Microtubule arrays present during syncytial blastoderm stage of the *Drosophila* embryo. Exp. Cell Res. *163*, 201–210.

Waters, J. C., Cole, R. W., and Rieder, C. L. (1993). The force-producing mechanism for centrosome separation during spindle formation in vertebrates is intrinsic to each aster. J. Cell Biol. *122*, 361–372.

Whitfield, W. G., Millar, S. E., Saumweber, H., Frasch, M., and Glover, D. M. (1988). Cloning of a gene encoding an antigen associated with the centrosome in *Drosophila*. J. Cell Sci. *89*, 467–480.

GenBank Accession Numbers

The accession numbers for the cDNA sequence and the genomic sequence of *aur* reported in this paper are X83465 and X83466, respectively.